

Investigating the Relationship Between Incineration Temperature, Rice Husk Ash (RHA) Characteristics, and Modified Asphalt Performance

Ya-ya ZUO¹, Xu-rong ZHANG¹, Li-yan JIN², Xin-xin CAO^{3*}

¹ Sichuan Chuangao Engineering Technology Consulting Co., Ltd, Chengdu, Sichuan, China

² Beijing Kuanmu Technology Co., Ltd, Beijing, China

³ School of Highway and Architecture, Shandong Transport Vocational College, Jinan, Shandong, China

<http://doi.org/10.5755/j02.ms.40698>

Received 3 March 2025; accepted 12 June 2025

Mixing rice husk ash into asphalt can not only avoid resource waste, but also improve the performance of asphalt. However, the incineration temperature of rice husk ash affects its activity, which in turn affects the performance of its modified asphalt. To investigate the influence of rice husk ash (RHA) prepared at different incineration temperatures on its properties and the performance of its modified asphalt, the amorphous SiO₂ content in RHA was determined using X-ray fluorescence spectrometry (XRF) and X-ray diffraction (XRD). Additionally, the microstructure of RHA was analyzed through scanning electron microscopy (SEM). RHA obtained at different incineration temperatures was utilized in the base asphalt as an additive to produce rice husk ash modified asphalt (RHAMA), and the high and low temperature performance, temperature sensitivity, and creep recovery of RHAMA were evaluated by the dynamic shear rheology (DSR) test, the bending beam rheology (BBR) test, and the multi-stress creep recovery (MSCR) test. These results were combined with microscopic analyses of RHA to assess the impact of incineration temperature on the performance of RHAMA. The findings reveal that when the calcination temperature exceeds 600 °C, the amorphous SiO₂ in RHA transitions to a crystalline phase. The incorporation of RHA enhances the high temperature performance and creep recovery of the base asphalt but reduces its temperature sensitivity and low temperature performance. As the incineration temperature of RHA increases, the high temperature performance and creep recovery of RHAMA decline, while temperature sensitivity and low temperature performance improve. The optimal calcination temperature for RHA is 600 °C, at which the amorphous SiO₂ content is maximized, resulting in the most significant improvement in the performance of the base asphalt.

Keywords: rice husk ash, incineration temperature, rice husk ash modified asphalt, high and low temperature performance, creep recovery performance.

1. INTRODUCTION

The increasing vehicle axle loads, rising traffic volumes, and construction or design errors contribute to various forms of asphalt pavement damage, including rutting, fatigue cracking, low temperature cracking, and water damage, all of which significantly reduce pavement serviceability [1]. These pavement distresses not only escalate road maintenance costs but also shorten the service life of roads. Asphalt, serving as the binding material in asphalt mixtures, plays a critical role in determining the mechanical properties of these mixtures and is directly linked to the occurrence of asphalt pavement diseases [2]. However, conventional matrix asphalt increasingly fails to meet the growing demands for road performance, necessitating its modification to effectively enhance the mechanical properties of asphalt mixtures. In recent years, a wide range of asphalt modifiers, including recycled rubber products, fillers, fibers, catalysts, polymers, and various additives, have been employed to improve the performance of matrix asphalt [3].

Amidst the growing scarcity of natural resources and increasingly severe environmental challenges, greater attention is being directed toward the utilization of industrial and agricultural waste materials [4]. Incorporating these

waste materials into asphalt pavements not only promotes resource recycling and conserves natural resources but also reduces project costs and minimizes environmental harm. Research has demonstrated that various waste materials, such as shells, reclaimed aggregates, glass, waste bricks, discarded tires, and recycled asphalt mixtures [5–9], have been successfully repurposed as aggregates, fillers, and modifiers in asphalt mixtures.

Rice is the most extensively cultivated crop globally, and rice husk, a significant by-product of rice processing, is often discarded due to its limited utilization potential [10]. Researchers have discovered that rice husk ash (RHA), produced after burning rice husk, contains 15 % to 20 % SiO₂ by weight. Under specific incineration conditions, the majority of the SiO₂ in RHA exists in an amorphous form, exhibiting high pozzolanic activity. This makes RHA an ideal candidate for use as a modifier or reinforcing agent in asphalt-based or cement-based materials [11, 12]. Despite its potential, the application of RHA in road engineering, particularly as an additive to asphalt, remains an emerging area of research. Alaaeldin et al. [13] demonstrated that RHA enhances the high temperature performance of asphalt. Furthermore, they found that a composite modification of asphalt using RHA and rubber particles outperformed

* Corresponding author: X. Cao

E-mail: 611200111008@mail.cqjtu.edu.cn

asphalt modified with either RHA or rubber particles alone. Lu et al. [14] utilized a mixture of RHA and styrene-butadiene-styrene (SBS) as a bio-additive to prepare SBS/RHA composite modified asphalt. Their study revealed that the viscosity and softening point of the modified asphalt increased with higher RHA content, while ductility decreased. Based on these findings, they recommended that the RHA dosage should not exceed 15 %. Xue et al. [15] compared RHA with woodchip ash and found that RHA provided superior improvements in the physical properties of asphalt. Fareed et al. [16] confirmed that RHA contains a significant amount of highly reactive amorphous SiO_2 , which, when used in modified asphalt, significantly enhances the resistance of asphalt mixtures to water damage, with negligible adverse effects on fatigue properties. Arabani et al. [17] reported that the incorporation of RHA improves the rheological properties of asphalt. Additionally, RHA positively influenced Marshall stability, strength modulus, high temperature stability, and fatigue properties of asphalt mixtures.

In summary, the use of RHA as an additive in modified asphalt has been shown to significantly enhance asphalt properties. To date, researchers have made substantial progress in the field of rice husk ash modified asphalt (RHAMA). However, limited attention has been given to the activity of RHA as a critical factor influencing the performance of modified asphalt. The activity of RHA is influenced by various preparation conditions, such as acid leaching treatment, heating rate, and incineration temperature [18, 19], and this activity directly impacts the performance of modified asphalt [20]. Among these factors, incineration temperature is the most significant [21]. Therefore, the study on the influence of incineration temperature of rice husk ash on its activity and the properties of modified asphalt is novel and necessary.

Building on this foundation, this study aims to explore the influence of RHA incineration temperature on its activity and the properties of modified asphalt. First, RHA was prepared under varying incineration temperature conditions. The amorphous SiO_2 content was determined using X-ray fluorescence (XRF) analysis and X-ray diffraction (XRD) patterns, while the microstructures of RHA were examined through scanning electron microscopy (SEM) images. Subsequently, RHA produced at different incineration temperatures was incorporated into base asphalt to produce RHAMA. The effects of RHA calcination temperature on the high- and low temperature performance, temperature sensitivity, and creep recovery properties of RHAMA were evaluated using dynamic shear rheology (DSR), bending beam rheology (BBR), and multi-stress creep recovery (MSCR) tests. The underlying mechanisms were analyzed by correlating these results with the microscopic test data of RHA. This research provides theoretical support for further enhancing the activity of RHA, offering significant insights into promoting the sustainable utilization of RHA in cementitious materials.

2. EXPERIMENTAL

2.1. Raw materials

The matrix asphalt used in this study was 70# base asphalt supplied by SK Energy in South Korea, with its key

performance indicators listed in Table 1. The rice husks were sourced locally from Harbin, Heilongjiang Province, and the hydrochloric acid used was a 5 % mass fraction dilute solution produced by Shanghai Sinopharm Group Chemical Reagent Co. Ltd., China.

Table 1. Main performance indicators of matrix asphalt

Norm	Penetration at 25 °C, 0.1 mm	Elongation at 10°C, cm	Softening point, °C	Density at 15°C, g/cm ³
Test results	66.2	24.1	47.0	1.027

2.2. Preparation of RHA and its modified asphalt

The preparation process of RHA is illustrated in Fig. 1. First, rice husks were immersed in a hydrochloric acid solution under constant stirring and soaked for 1 h to thoroughly remove impurities. The acid-treated rice husks were then rinsed repeatedly with distilled water until the rinsing solution reached a neutral pH. After rinsing, the rice husks were dried in an oven. Subsequently, the dried rice husks were calcined in a muffle furnace for 2 h at temperatures of 600 °C, 700 °C, and 800 °C. To prevent the transformation of amorphous SiO_2 into a crystalline state, the calcined rice husks were rapidly cooled in an ice-water mixture at 0 °C. Finally, the cooled rice husks were dried and ground into a fine powder, yielding RHA samples calcined at 600 °C, 700 °C, and 800 °C, respectively.

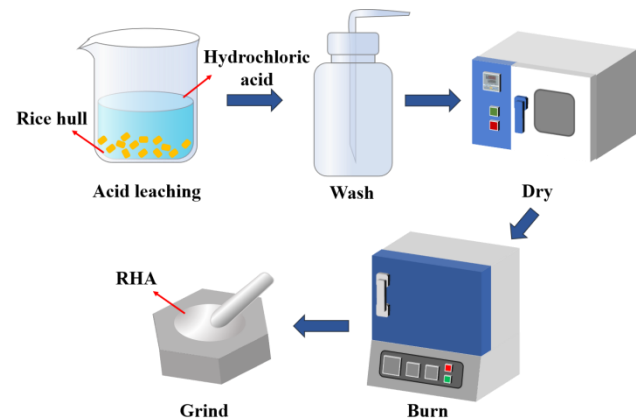


Fig. 1. Preparation process of RHA

Research has demonstrated that the application of RHA in modified asphalt is not optimal at higher dosages; rather, a dosage ratio of approximately 7 % (by mass of the matrix asphalt) results in RHAMA with superior performance [10, 13, 14, 16, 17]. Therefore, in this study, RHAMA was prepared using an RHA dosage of 7 % (by mass of the matrix asphalt). The preparation process of RHAMA is illustrated in Fig. 2. First, the matrix asphalt was heated to a flowing state, and a measured amount was poured into a beaker. The beaker was then placed in a 160 °C oil bath for temperature control. Next, the pre-weighed RHA was added to the beaker, and the mixture was thoroughly stirred. High-speed shearing was initiated at a rate of 5,000 rpm for 30 minutes, followed by a 1 h solubilization period. Finally, the RHAMA was obtained. The matrix asphalt and RHAMA mixed with RHA calcined at 600 °C, 700 °C, and 800 °C were labeled as samples a, b, c, and d, respectively.

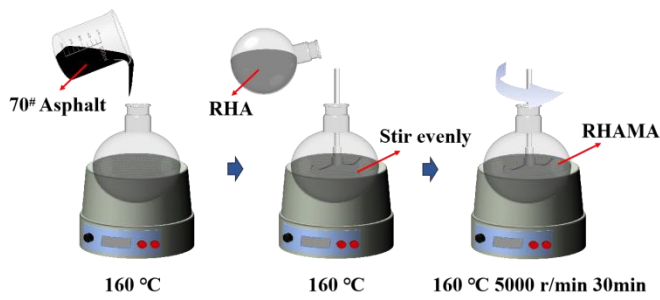


Fig. 2. Preparation process of RHAMA

2.3. Experimental methodology

2.3.1. X-ray fluorescence spectroscopy (XRF)

The chemical composition of RHA at different calcination temperatures was determined using an X-ray fluorescence spectrometer (ZSX primus II) manufactured by Rigaku, Japan.

2.3.2. X-ray diffraction (XRD)

The crystal structure of RHA was characterised using an X-ray diffractometer (D8 ADVANCE) from Bruker, Germany, in order to analyse the effect of calcination temperature on the amorphous SiO_2 content of RHA, with a scanning range of $2\theta = 5^\circ \sim 80^\circ$ and a scanning speed of $5^\circ/\text{min}$.

2.3.3. Scanning electron microscope

The microscopic morphology and structure of RHA were observed by a field emission scanning electron microscope (Inspect S50) manufactured by FEI, USA, with an accelerating voltage of 20 kV, and the surface of the sample was sprayed with gold.

2.3.4. Dynamic shear rheology test

The high temperature rheological properties of RHAMA samples were investigated using a DHR-2 dynamic shear rheometer manufactured by TA, USA. The test method refers to AASHTO T315-2008, a circular rotor with a diameter of 25 mm and a spacing of 1 mm between the plates was used. The sample was first heated to a fluid state and then poured into a polytetrafluoroethylene mould, and then the sample was cooled to a solid state and taken out for use, as shown in Fig. 3.

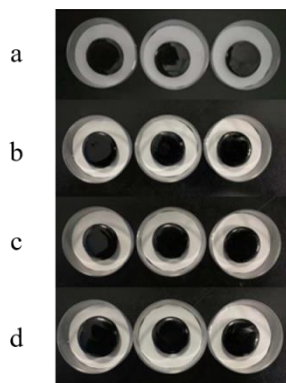


Fig. 3. DSR test samples

The sample was then placed between the plates of the instrument, and the temperature scanning test was started

after the heat preservation was completed. The temperature interval was from 46°C to 76°C with a temperature gradient of 6°C .

2.3.5. Bending beam rheology test

The low temperature properties of RHAMA were determined using a WBBR-3Pro type bending beam rheometer produced by Hunan Wangxuan Technology Co. Ltd., China. The test method was based on the relevant provisions in AASHTO T313-2009, and the test temperatures were set at -12°C , -18°C and -24°C .

2.3.6. Multi-stress creep recovery test

A dynamic shear rheometer of the same type as the DSR test and the sample preparation method were used, and the test method was referred to AASHTO T350-2014, a circular rotor with a diameter of 25 mm was selected, the clearance between the rotor and the steel plate was 1 mm, the shear stresses were taken as 0.1 kPa versus 3.2 kPa, and the temperature intervals were set from 46°C to 76°C , with an interval of 6°C . The rheological behaviour of RHAMA was tested for 10 cycles of shear stress. Each cycle was 10 s, including 1 s of creep phase and 9 s of recovery phase.

3. TEST RESULTS AND ANALYSIS

3.1. Compositional analysis of RHA

3.1.1. Chemical composition of RHA

The chemical composition of RHA prepared at different calcination temperatures is shown in Table 2.

Table 2. Chemical composition of RHA (mass content, %)

Calcination temperature	SiO_2	Al_2O_3	Na_2O	P_2O_5	CaO	MgO
600°C	94.57	1.21	0.21	0.22	0.35	0.92
700°C	94.74	1.41	0.22	0.21	0.33	0.85
800°C	94.78	1.24	0.21	0.22	0.36	0.80

From the XRF test results, it is evident that the primary component of RHA is SiO_2 , constituting approximately 95 % of the total mass of the rice husk. The SiO_2 content remains unaffected by variations in calcination temperature. Additionally, RHA contains trace amounts of metal oxides and phosphides, indicating that the acid leaching pretreatment effectively removes impurities, leaving minimal residual contaminants.

3.1.2. Crystal structure analysis of RHA

The XRD patterns of RHA prepared at different calcination temperatures are shown by Fig. 4. As shown in curve a of Fig. 1, a broad and relatively flat raised peak appears between $2\theta = 18^\circ$ and 28° , which is the characteristic peak of amorphous SiO_2 . This indicates that at a calcination temperature of 600°C , the SiO_2 in RHA predominantly exists in an amorphous form [22]. Near $2\theta \approx 22^\circ$, curves b and c exhibit a narrow and sharp peak of similar height, representing the characteristic peak of crystalline SiO_2 . This suggests that at calcination temperatures of 700°C or higher, the amorphous SiO_2 in RHA undergoes a crystalline transformation, converting into crystalline phases such as cristobalite and tridymite

[22, 23]. Additionally, near $2\theta \approx 37^\circ$, curves b and c display a sharp peak with relatively low intensity, which may correspond to the crystalline transformation of other impurities present in the rice husk.

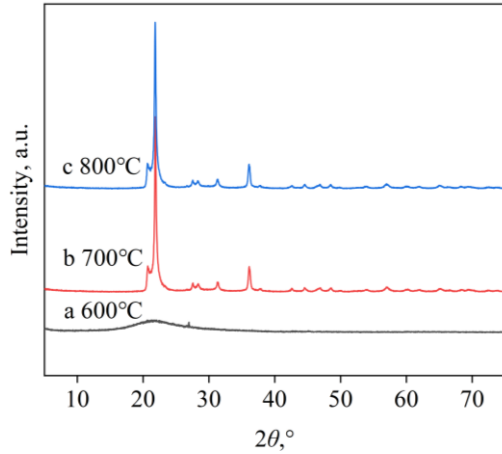


Fig. 4. XRD patterns of RHA at different incineration temperatures

Based on the XRF test results and XRD pattern analysis of RHA at different calcination temperatures, it is evident that at a calcination temperature of 600 °C, the majority of SiO_2 in RHA exists in an amorphous state, with a content of approximately 94.57 %. However, when the calcination temperature exceeds 600 °C, the amorphous SiO_2 in RHA undergoes a crystalline phase transition. To maximize the content of highly active amorphous SiO_2 and align with energy-saving and emission-reduction goals, the optimal calcination temperature for RHA should be 600 °C.

3.1.3. Microstructural analysis of RHA

SEM images of RHA prepared at calcination temperatures of 600 °C, 700 °C, and 800 °C are shown in Fig. 5. From the SEM images of RHA after calcination, it is observed that at a calcination temperature of 600 °C, RHA exhibits a large specific surface area with a distinct laminar structure. When the calcination temperature increases to 700 °C, the laminar structure of RHA transforms into depressions and aggregates, with some depressions forming a cross-linking structure. As the calcination temperature rises further to 800 °C, the laminar structure in RHA completely disappears and is replaced by irregularly shaped spheres. The surfaces of these spheres are covered by dense SiO_2 films, indicating that the amorphous SiO_2 in RHA gradually transitions into crystalline SiO_2 as the calcination temperature increases.

3.2. Performance analysis of RHAMA

3.2.1. High temperature performance

The DSR test simulates the forces exerted on asphalt in real pavement conditions by measuring the torque required during rotation and the shear strain of the asphalt. From these measurements, the complex modulus (G^*) and phase angle (δ) of the asphalt can be calculated to evaluate its rheological properties. G^* and δ together characterize the viscoelastic behavior of the asphalt. The complex modulus G^* comprises the storage modulus ($G' = G \cos \delta$), representing the elastic component, and the loss modulus ($G'' = G \sin \delta$), representing the viscous component.

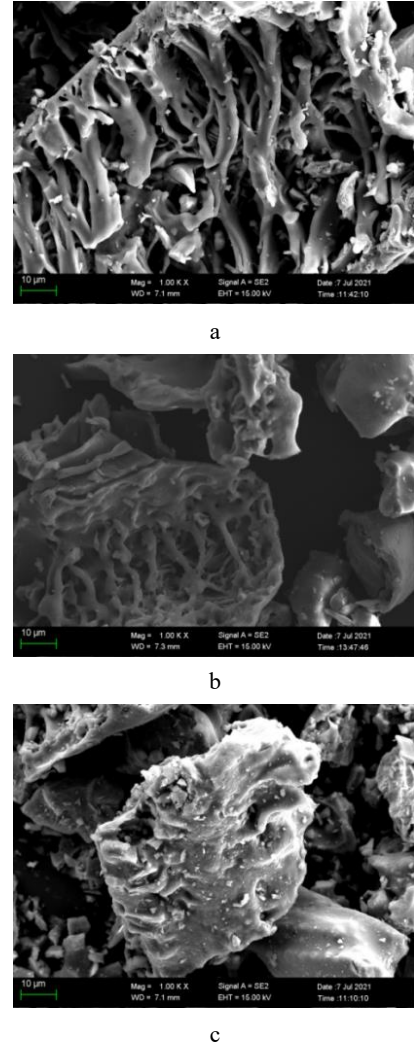


Fig. 5. SEM images of RHA with different calcination temperatures: a–600 °C; b–700 °C; c–800 °C

A smaller δ indicates that the asphalt exhibits more elastic behavior, suggesting greater resistance to deformation at high temperatures. Conversely, a larger δ reflects higher viscosity in the asphalt. Additionally, higher G^* values combined with lower δ values indicate superior rutting resistance of the asphalt [24, 25]. The results of the DSR test for RHAMA are presented in Fig. 6. As shown in Fig. 6 a and b, at the same test temperature, the complex shear modulus of RHAMA is significantly higher than that of the base asphalt, while the phase angle of RHAMA is notably lower. This indicates that the incorporation of RHA enhances the high temperature performance of the asphalt. The improvement can be attributed to the porous structure of RHA, which absorbs the asphalt, strengthens the bonding between asphalt particles, and acts as a filler and reinforcing agent. These mechanisms collectively enhance the asphalt's resistance to high temperature deformation.

Additionally, as observed in Fig. 6 a and b, the high temperature performance of RHAMA decreases as the incineration temperature of RHA increases. This demonstrates that the incineration temperature of RHA significantly influences the high temperature performance of the modified asphalt. As the incineration temperature rises, the amorphous SiO_2 in RHA gradually loses its activity and transforms into crystalline SiO_2 . This transition

weakens the adsorption capacity of RHA on the asphalt, thereby reducing the high temperature performance of the asphalt.

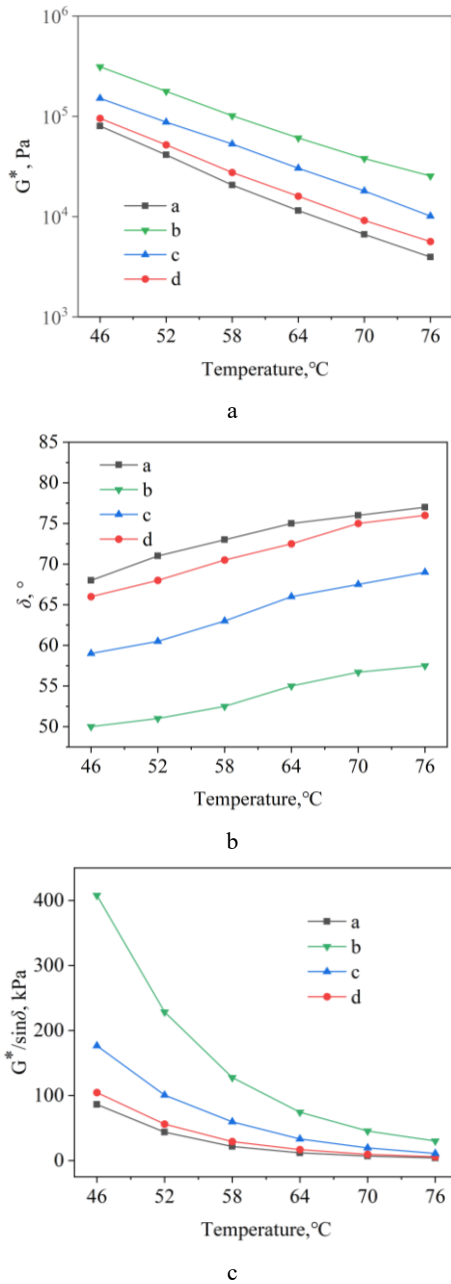


Fig. 6. DSR test results of RHAMA: a—complex modulus; b—phase angle; c—rutting factor

The rutting factor ($G^*/\sin\delta$) is used in the Superpave specification as an indicator of the resistance to permanent deformation in asphalt materials, serving as a key parameter to characterize high temperature performance. Fig. 6 c illustrates the relationship between the rutting factor and temperature for RHAMA. The results reveal that the rutting factor of RHAMA is significantly higher than that of the base asphalt at the same test temperature. This further confirms that RHA enhances the high temperature rheological properties of asphalt and improves its resistance to rutting. Moreover, within RHAMA, the rutting factor decreases as the incineration temperature of RHA increases. This indicates that higher incineration temperatures reduce

the activity of RHA, diminishing its interaction with the asphalt and consequently lowering the high temperature rutting resistance of the modified asphalt.

3.2.2. Temperature sensitivity

The temperature sensitivity of asphalt refers to the extent to which its properties change with variations in temperature. When asphalt exhibits low temperature sensitivity, it indicates relatively minor changes in its properties across different temperatures, reflecting better thermal stability and temperature adaptability [26]. To evaluate the temperature sensitivity of RHAMA, the complex modulus index is used. This index is calculated by taking the logarithm of the complex modulus twice and then determining the slope of the curve representing the logarithmic change with respect to temperature. A smaller absolute value of the complex modulus index corresponds to lower temperature sensitivity in the asphalt. The complex modulus index was calculated as

$$\lg \lg G^* = GTS \times \lg T + C, \quad (1)$$

where GTS is the complex modulus index; G^* is the complex modulus, Pa; T is the test temperature, K; C is the constant. The results of the asphalt temperature sensitivity analysis at each RHA dosage are shown in Table 3.

Table 3. Complex modulus index of RHAMA

Groups	GTS	C	R^2
a	-3.4590	9.3523	0.9998
b	-2.4811	6.9524	0.9995
c	-2.8395	7.8271	0.9949
d	-3.1705	8.6372	0.9996

As shown in Table 3, the R^2 value for asphalt at each RHA dosage exceeds 0.99, indicating a strong correlation between the complex modulus and temperature. The incorporation of RHA reduces the absolute value of the GTS , suggesting that the slope of the complex modulus versus temperature curve for RHAMA decreases, resulting in lower temperature sensitivity. This is attributed to the physical filling effect of RHA particles, which act as microaggregates within the asphalt, increasing its density and strength. This effect enhances the asphalt's resistance to high temperature deformation, thereby reducing its temperature sensitivity. Additionally, Table 3 reveals that the incineration temperature of RHA also influences the GTS value of the modified asphalt. As the incineration temperature of RHA increases, the absolute value of the GTS for the modified asphalt gradually rises, indicating higher temperature sensitivity. This occurs because RHA incinerated at 600 °C contains a significant number of active components, such as amorphous SiO_2 , which undergo chemical reactions with the asphalt colloids to form more stable macromolecular compounds. These compounds have high melting points and strong adhesion, making RHAMA less prone to flow and deformation at high temperatures, thereby reducing temperature sensitivity. However, as the incineration temperature of RHA increases, the amorphous SiO_2 within RHA gradually transforms into a crystalline phase, which only interacts with the base asphalt through physical adsorption. This reduces the effectiveness of RHA in

improving the temperature sensitivity of RHAMA.

3.2.3. Low temperature performance

The asphalt low temperature bending beam rheology (BBR) test, developed under the U.S. Strategic Highway Research Program (SHRP), is a widely used method to evaluate the low temperature performance of asphalt materials. This test typically employs two key parameters: the creep stiffness modulus (S) and the creep rate (m). The creep stiffness (S) reflects the flexibility of asphalt materials at low temperatures, with lower values of S indicating greater flexibility. The creep rate (m) describes the rate of change in stiffness over time and characterizes the stress relaxation capability of asphalt materials at low temperatures, where higher values of m indicate better stress relaxation capacity [27]. The results of the BBR test for RHAMA are presented in Fig. 7.

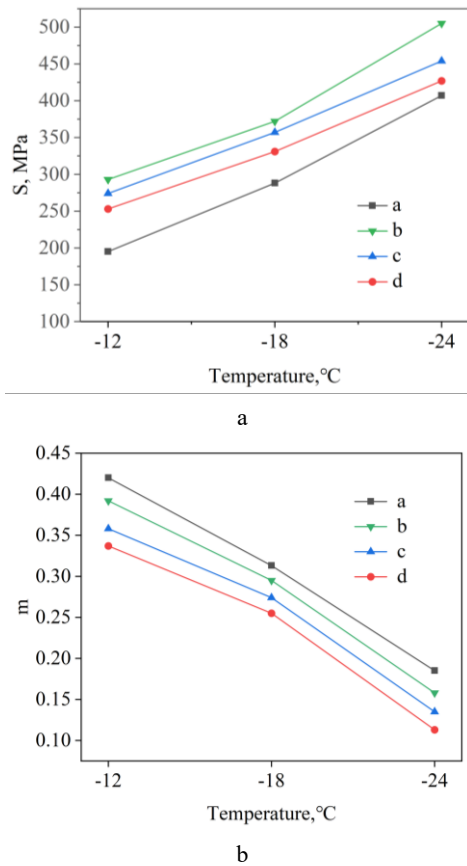


Fig. 7. BBR test results of RHAMA: a – creep stiffness modulus; b – creep rate

As illustrated in Fig. 7, at identical test temperatures, the creep stiffness modulus of RHAMA is significantly higher than that of the base asphalt, while its creep rate is markedly lower. The incorporation of RHA tends to compromise the low temperature performance of the asphalt. This phenomenon can be attributed to the fact that the addition of RHA reduces the fluidity of the asphalt through adsorption. The interaction between RHA and asphalt forms a mesh structure that increases the ash content, thereby enhancing the brittleness of the asphalt and consequently diminishing its low temperature performance.

Furthermore, Fig. 7 reveals that the low temperature performance of RHAMA improves as the incineration

temperature of RHA increases. This improvement is due to the presence of a substantial amount of amorphous SiO_2 in RHA incinerated at 600 °C, which exhibits excellent volcanic ash activity. This amorphous SiO_2 is effectively adsorbed into the asphalt matrix, further impairing the asphalt's low temperature performance. However, as the incineration temperature of RHA rises, the amorphous SiO_2 gradually transforms into a crystalline phase structure, leading to a loss of RHA activity. This transformation weakens the interaction between RHA and asphalt, reduces the ash content, and ultimately restores the low temperature performance of the asphalt.

3.2.4. Creep recovery performance

The creep recovery performance of asphalt refers to its ability to revert to its original shape after the removal of an external force following creep deformation under a constant load. This property is crucial as it directly influences the durability and stability of asphalt pavements. The MSCR test is a widely used method to assess the strain recovery capability of asphalt materials under specific temperature conditions and varying stress levels. The MSCR test results for RHAMA are presented in Fig. 8.

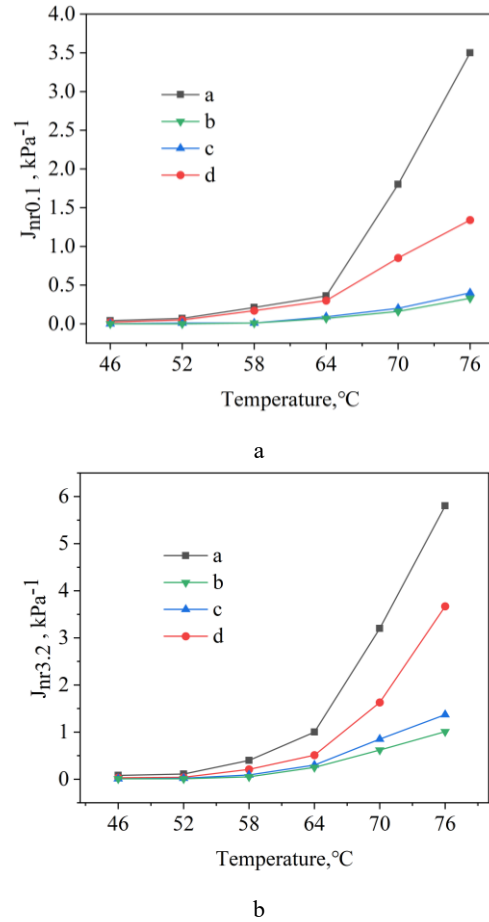


Fig. 8. MSCR test results of RHAMA: a – 0.1 kPa; b – 3.2 kPa

The average unrecoverable creep compliance ($J_{nr3.2}$ and $J_{nr0.1}$) reflects the cumulative deformation of asphalt pavement under high temperature traffic loading within a single cycle. Higher values of $J_{nr3.2}$ and $J_{nr0.1}$ indicate poorer creep recovery performance, while lower values signify better creep recovery performance of the asphalt pavement [28].

As shown in Fig. 8, at the same test temperature, the incorporation of RHA reduces the average unrecoverable creep compliance of asphalt and enhances its creep recovery performance. This improvement can be attributed to the role of RHA as fine particles that fill the voids within the asphalt, increasing its density and thereby improving its resistance to creep deformation. Additionally, RHA particles act as physical barriers, restricting the free movement of asphalt molecules and reducing the likelihood of creep deformation. When the test temperature reaches 64 °C, the creep recovery performance of the asphalt material reaches a turning point. This is because, under high-temperature conditions, the molecular chain mobility of the asphalt material increases, the internal frictional resistance decreases, and the material becomes more prone to irreversible plastic deformation.

Furthermore, Fig. 8 indicates that the creep recovery performance of RHAMA decreases as the incineration temperature of RHA increases. This is due to the high reactivity of RHA incinerated at 600 °C. The active components in RHA can chemically react with certain components in asphalt, forming new chemical bonds that enhance intermolecular interactions and improve creep resistance [29]. However, as the incineration temperature rises, the reactivity of RHA diminishes, reducing its ability to chemically interact with the asphalt and consequently weakening the creep recovery performance. Some studies [30, 31] suggest that for pavements subjected to extremely heavy traffic, the J_{nr} value should be less than 0.5 kPa^{-1} . As seen in Fig. 8, RHAMA prepared with RHA incinerated at temperatures below 700 °C meets the requirements for extremely heavy traffic at high temperatures of 64 °C.

4. CONCLUSIONS

The purpose of this study is to investigate the effect of RHA incineration temperature on its activity and its modified asphalt properties. Firstly, RHA under different incineration temperature conditions was prepared, and the amorphous SiO_2 content was calculated by using the results of XRF analysis and XRD patterns, and the microstructure of RHA was observed by SEM images. Then the RHA with different incineration temperatures was blended into the matrix asphalt to obtain the RHAMA. The effects of RHA incineration temperature on the high and low temperatures, temperature sensitivity and creep recovery properties of RHAMA were investigated by DSR, BBR and MSCR tests. The main research conclusions are as follows:

1. The XRF test results and XRD patterns reveal that when the calcination temperature is 600 °C, the majority of SiO_2 in the RHA exists in an amorphous state, accounting for approximately 94.57 %. However, when the calcination temperature exceeds 600 °C, the amorphous SiO_2 in the RHA undergoes a phase transition to a crystalline structure.
2. SEM images of RHA revealed that when rice husk was calcined at 600 °C, the SiO_2 in RHA predominantly exhibited an amorphous form with a distinct laminar structure. As the calcination temperature increased, the amorphous SiO_2 in RHA underwent a crystalline phase transition, resulting in a transformation of its microstructure from a laminar structure to irregular spherical particles. Additionally, the surface of these

particles was covered by a dense SiO_2 film.

3. The incorporation of RHA significantly improves the high temperature performance and creep recovery properties of the base asphalt. However, in RHAMA, as the incineration temperature of RHA increases, the amorphous SiO_2 within RHA gradually loses its reactivity and transforms into crystalline SiO_2 . This transition weakens the adsorption capacity of RHA on the asphalt, thereby reducing both the high temperature performance and creep recovery performance of the modified asphalt.
4. The incorporation of RHA reduced the temperature sensitivity and low temperature performance of the base asphalt. However, in RHAMA, as the incineration temperature of RHA increased, the activity of RHA gradually diminished. This led to a weakening of the interaction between RHA and asphalt, a reduction in the ash content, and a subsequent recovery of the asphalt's temperature sensitivity and low temperature performance.
5. Based on the experimental analysis, it is evident that the optimal calcination temperature for rice husk is 600 °C. At this temperature, the resulting RHA contains the highest proportion of amorphous SiO_2 , which significantly enhances the high temperature performance, thermal stability, and creep recovery properties of the base asphalt

Acknowledgments

The research was funded by the basic scientific research of the central institute (2021-9003a) and the ongoing research projects of the National Natural Science Foundation of China (51908260). That sponsorship and interest are gratefully acknowledged.

REFERENCES

1. Sengoz, B., Topal, A. Use of Asphalt Roofing Shingle Waste in HMA *Construction and Building Materials* 19 (5) 2005: pp. 337–346.
<https://doi.org/10.1016/j.conbuildmat.2004.08.005>
2. Lesueur, D. The Colloidal Structure of Asphalt: Consequences on the Rheology and on the Mechanisms of Bitumen Modification *Advances in Colloid and Interface Science* 145 (1–2) 2009: pp. 42–82.
<https://doi.org/10.1016/j.cis.2008.08.011>
3. Rusbintardjo, G., Hainin, M.R., Yusoff, N.I.M. Fundamental and Rheological Properties of Oil Palm Fruit Ash Modified Bitumen. *Construction and Building Materials* 49 2013: pp. 702–711.
<https://doi.org/10.1016/j.conbuildmat.2013.08.056>
4. Arabani, M., Tahami, S.A., Taghipoor, M. Laboratory Investigation of Hot Mix Asphalt Containing Waste Materials *Road Materials and Pavement Design* 18 (3) 2016: pp. 713–729.
<https://doi.org/10.1080/14680629.2016.1189349>
5. Guo, Y.C., Wang, X.C., Ji, G.Y., Zhang, Y., Su, H., Luo, Y.L. Effect of Recycled Shell Waste as a Modifier on the High and Low Temperature Rheological Properties of Asphalt *Sustainability* 13 (18) 2021: pp. 10271.
<https://doi.org/10.3390/su131810271>
6. Arabani, M., Babamohammadi, S., Azarhoosh, A.R. Experimental Investigation of Seashells Used as Filler in Hot Mix Asphalt *International Journal of Pavement Engineering* 16 (6) 2015: pp. 502–509.

<https://doi.org/10.1080/10298436.2014.943132>

7. **Gómez-Meijide, B., Pérez, I., Airey, G., Thom, N.** Stiffness of Cold Asphalt Mixtures with Recycled Aggregates from Construction and Demolition Waste. *Construction and Building Materials* 77 2015: pp. 168–178. <https://doi.org/10.1016/j.conbuildmat.2014.12.045>
8. **Arabani, M., Tahami, S.A., Hamed, G.H.** Performance Evaluation of Dry Process Crumb Rubber-Modified Asphalt Mixtures with Nanomaterial. *Road Materials and Pavement Design* 19 (5) 2017: pp. 1241–1258. <https://doi.org/10.1080/14680629.2017.1302356>
9. **Huang, B.S., Shu, X., Vukosavljevic, D.** Laboratory Investigation of Cracking Resistance of Hot-Mix Asphalt Field Mixtures Containing Screened Reclaimed Asphalt Pavement. *Journal of Materials in Civil Engineering* 23 (11) 2010: pp. 1535–1543. [https://doi.org/10.1061/\(ASCE\)MT.1943-5533.0000223](https://doi.org/10.1061/(ASCE)MT.1943-5533.0000223)
10. **Abdelmagid, A.A.A., Qiu, Y., Yang, E.** Using Agricultural Residue Sustainably: Enhancing Asphalt Properties with Rice Husk Ash and Analyzing Its Mixture Performance Using Response Surface Methodology. *Case Studies in Construction Materials* 19 2023: pp. e02476. <https://doi.org/10.1016/j.cscm.2023.e02476>
11. **Camargo-Perez, R., Moreno-Navarro, F., Alvarez, A.E., Walubita, L.F., Fuentes, L.** Influence of Recycled Rice Husk Ash Filler on the Mechanical Performance of Asphalt Mixtures: A Mortar Scale Analysis. *Construction and Building Materials* 414 2024: pp. 134832. <https://doi.org/10.1016/j.conbuildmat.2024.135316>
12. **Hu, L.L., He, Z., Zhang, S.P.** Sustainable Use of Rich Husk Ash in Cement-Based Materials: Environmental Evaluation and Performance Improvement. *Journal of Cleaner Production* 264 2020: pp. 121744. <https://doi.org/10.1016/j.jclepro.2020.121744>
13. **Alaeldin, A.A.A., Cheng, P.F.** Evaluating the Effect of Rice-Husk Ash and Crumb-Rubber Powder on the High Temperature Performance of Asphalt Binder. *Journal of Materials in Civil Engineering* 31 (12) 2019: pp. 04019296. [https://doi.org/10.1061/\(ASCE\)MT.1943-5533.0002962](https://doi.org/10.1061/(ASCE)MT.1943-5533.0002962)
14. **Lu, Z., Sha, A., Wang, W., Gao, J.** Studying the Properties of SBS/Rice Husk Ash-Modified Asphalt Binder and Mixture. *Advances in Materials Science and Engineering* 2020 2020: pp. 4545063. <https://doi.org/10.1155/2020/4545063>
15. **Xue, Y.J., Wu, S.P., Cai, J., Zhou, M., Zha, J.** Effects of Two Biomass Ashes on Asphalt Binder: Dynamic Shear Rheological Characteristic Analysis. *Construction and Building Materials* 56 2014: pp. 7–15. <https://doi.org/10.1016/j.conbuildmat.2014.01.075>
16. **Fareed, A., Zaidi, S.B.A., Ahmad, N., Hafeez, I., Ali, A., Ahmad, M.F.** Use of Agricultural Waste Ashes in Asphalt Binder and Mixture: A Sustainable Solution to Waste Management. *Construction and Building Materials* 259 2020: pp. 120575. <https://doi.org/10.1016/j.conbuildmat.2020.120575>
17. **Arabani, M., Tahami, S.A.** Assessment of Mechanical Properties of Rice Husk Ash Modified Asphalt Mixture. *Construction and Building Materials* 149 2017: pp. 350–358. <https://doi.org/10.1016/j.conbuildmat.2017.05.127>
18. **Hoppe-Filho, J., Garcez, M.R., Medeiros, M.H.F., Silva-Filho, L.C.P., Isaia, G.C.** Reactivity Assessment of Residual Rice-Husk Ashes. *Journal of Materials in Civil Engineering* 29 (6) 2017: pp. 04017003. [https://doi.org/10.1061/\(ASCE\)MT.1943-5533.0001820](https://doi.org/10.1061/(ASCE)MT.1943-5533.0001820)
19. **Zain, M.F.M., Islam, N.M., Mahmud, F., Jamil, M.** Production of Rice Husk Ash for Use in Concrete as a Supplementary Cementitious Material. *Construction and Building Materials* 25 (2) 2011: pp. 798–805. <https://doi.org/10.1016/j.conbuildmat.2010.07.003>
20. **Mistry, R., Roy, T.K.** Performance Evaluation of Bituminous Mix and Mastic Containing Rice Husk Ash and Fly Ash as Filler. *Construction and Building Materials* 268 2021: pp. 121187. <https://doi.org/10.1016/j.conbuildmat.2020.121187>
21. **Shen, J.F., Liu, X.Z., Zhu, S.G., Zhang, H.L., Tan, J.J.** Effects of Calcination Parameters on the Silica Phase of Original and Leached Rice Husk Ash. *Materials Letters* 65 (8) 2011: pp. 1179–1183. <https://doi.org/10.1016/j.matlet.2011.01.034>
22. **Ahmed, A.E., Adam, F.** Indium Incorporated Silica From Rice Husk and Its Catalytic Activity. *Microporous and Mesoporous Materials* 103 (1–3) 2007: pp. 284–295. <https://doi.org/10.1016/j.micromeso.2007.01.055>
23. **Nehdi, M., Duquette, J., Damatty, A.E.** Performance of Rice Husk Ash Produced Using a New Technology as a Mineral Admixture in Concrete. *Cement and Concrete Research* 33 (8) 2003: pp. 1203–1210. [https://doi.org/10.1016/S0008-8846\(03\)00038-3](https://doi.org/10.1016/S0008-8846(03)00038-3)
24. **Ghasemirad, A., Bala, N., Hashemian, L.** High Temperature Performance Evaluation of Asphaltene-Modified Asphalt Binders. *Molecules* 25 (15) 2020: pp. 3326. <https://doi.org/10.3390/molecules25153326>
25. **Xie, C., Luo, J.H., Zeng, L.H., Ren, T.Z., Liu, H.B., Chen, J.C.** Research on Evaluation Index of High Temperature Performance of Rubberized Asphalt Binder. *Frontiers in Materials* 9 2022: pp. 904087. <https://doi.org/10.3389/fmats.2022.904087>
26. **Yin, P., Pan, B.F.** Evaluation of Temperature Sensitivity of Recycled Asphalt Based on Numerical Analysis Model and Thermal Analysis Kinetics. *Construction and Building Materials* 344 2022: pp. 128153. <https://doi.org/10.1016/j.conbuildmat.2022.128153>
27. **Wang, T., Wang, J.Y., Hou, X.D., Xiao, F.P.** Effects of SARA Fractions on Low Temperature Properties of Asphalt Binders. *Road Materials and Pavement Design* 22 (3) 2019: pp. 539–556. <https://doi.org/10.1080/14680629.2019.1628803>
28. **Li, Z.H., Cao, X.J., Li, J., Yang, X.Y., Huang, C.** Preparation and Characterization of Bio-Asphalt Based on Sludge-Derived Heavy Oil. *Coatings* 14 (8) 2024: pp. 992. <https://doi.org/10.3390/coatings14080992>
29. **Han, Z.Q., Sha, A.M., Tong, Z., Liu, Z.Z., Gao, J., Zou, X.L., Yuan, D.D.** Study on the Optimum Rice Husk Ash Content Added in Asphalt Binder and Its Modification with Bio-Oil. *Construction and Building Materials* 147 2017: pp. 776–789. <https://doi.org/10.1016/j.conbuildmat.2017.05.004>
30. **DuBois, E., Mehta, D., Nolan, A.** Correlation between Multiple Stress Creep Recovery (MSCR) Results and Polymer Modification of Binder. *Construction and Building Materials* 65 2014: pp. 184–190. <https://doi.org/10.1016/j.conbuildmat.2014.04.111>
31. **Shirodkar, P., Mehta, Y., Nolan, A., Dahm, K., Dusseau, R., McCarthy, L.** Characterization of Creep and Recovery Curve of Polymer Modified Binder. *Construction and Building Materials* 34 2012: pp. 504–511. <https://doi.org/10.1016/j.conbuildmat.2012.02.018>

